Molecular Crystals and Liquid Crystals

ISSN: 1542-1406 (Print) 1563-5287 (Online) Journal homepage: http://www.tandfonline.com/loi/gmcl20

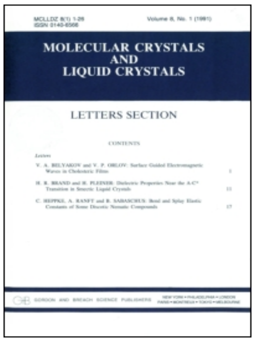

Synthesis of vinyl-functionalized azobenzene mesogens and study of their liquid-crystalline behavior

Marco De Jesús Téllez, Dámaso Navarro-Rodríguez & Leticia Larios-Lopez

To cite this article: Marco De Jesús Téllez, Dámaso Navarro-Rodríguez & Leticia Larios-Lopez (2017) Synthesis of vinyl-functionalized azobenzene mesogens and study of their liquid-crystalline behavior, Molecular Crystals and Liquid Crystals, 647:1, 269-278, DOI: 10.1080/15421406.2017.1289607

To link to this article: http://dx.doi.org/10.1080/15421406.2017.1289607

MOLECULAR CRYSTALS AND LIQUID CRYSTALS
2017, VOL. 647, 269–278
http://dx.doi.org/10.1080/15421406.2017.1289607

Synthesis of vinyl-functionalized azobenzene mesogens and study of their liquid-crystalline behavior

Marco De Jesús Téllez, Dámaso Navarro-Rodríguez, and Leticia Larios-Lopez

Departamento de Materiales Avanzados, Centro de Investigación en Química Aplicada. Blvd. Enrique Reyna, Saltillo Coahuila, México

ABSTRACT
Four vinyl-functionalized azobenzene-based liquid crystals (LCs) were synthesized and characterized by ^{1}H and ^{13}C nuclear magnetic resonance, and Fourier transform infrared spectroscopies. Their thermal stability was measured by thermogravimetric analysis and their thermotropic liquid-crystalline properties were determined by differential scanning calorimetry (DSC), polarized optical microscopy (POM), and X-ray diffraction (XRD). The azobenzene-based LCs displayed a nematic phase whereas those mesogens having an extra phenyl group developed lamellar mesophases of the SmA and SmC types. Combined with non-photoactive monomers, these vinyl-functionalized azobenzene-based mesogens can be used to prepare photo-active side-chain liquid crystal elastomers having potential use in optical actuators.

KEYWORDS
Azobenzene-based mesogen; vinyl-functionalized; photosensitive liquid crystal

1. Introduction

Liquid crystals (LCs) are mesomorphic materials possessing orientational and/or long-range positional order like solids, and fluidity like liquids. The combination of these two characteristics in LCs makes them unique and suitable for specific technological applications, some of them considered revolutionary. Most liquid crystals are anisotropic organic compounds (known as mesogens) combining a rigid core that is often composed of aromatic rings, and one or more alkyl chains; the former is able to interact through strong intermolecular π-bonds whereas the latter is flexible and can disrupt to some extent such interactions [1,3]. Among the wide variety of mesogens, the alkyl-substituted azobenzenes have attracted great attention due to their unique and remarkable response (photo-isomerization and photo-orientation) to light stimuli in the UV-vis wavelengths, and that find use in a variety of applications, including optical data storage memories, artificial muscles, molecular rotary motors, micro-pumps, autonomous valves, among others [4,5]. Azobenzene groups can be easily modified with specific terminal and lateral groups to induce either small structural changes to finely adjust the mesomorphic and optical response, or big changes to produce a significant modification in such properties or to induce new and sometimes unexpected properties [6].

CONTACT Leticia Larios-Lopez ✉ leticia.larios@ciqa.edu.mx Departamento de Materiales Avanzados, Centro de Investigación en Química Aplicada. Blvd. Enrique Reyna 140, C.P. 25294, Saltillo Coahuila, México.
Color versions of one or more of the figures in the article can be found online at www.tandfonline.com/gmcl.

Azobenzene liquid crystals carrying a vinyl group are "*reactive mesogens*" that can be used to prepare polymers and copolymers also showing liquid crystal and photo-responsive properties [7]. Lee and White employed vinyl-functionalized azobenzene mesogens to synthesize liquid crystal networks (LCN), which were evaluated in their photo-mechanical, photochemical and photothermal responses [8]. García-Amoros et al. used vinyl cyano-azobenzene mesogens (5 wt%) to prepare side-chain liquid crystal elastomers for which the photo-actuation and thermal isomerization mechanisms were studied [9]. Despite the relative low content of azo-mesogens, these elastomers were reported to exhibit a contraction along de director direction as an effect of the *trans-cis* photo-conversion of azobenzene groups. Herein, the synthesis and the liquid-crystalline behavior of four vinyl-functionalized liquid crystals are studied. These materials will be further used for the preparation of side-chain liquid crystal elastomers that are able of exhibiting photo and thermal-actuation.

2. Experimental

2.1. Materials

Reagents and solvents were purchased from Aldrich and/or J. T. Baker, and used as received, except for tetrahydrofurane (THF), which was dried and distilled from a sodium/benzophenone complex immediately prior to use.

2.2. Synthesis

Four vinyl-functionalized azobenzene mesogens were synthesized following the general route outlined in Figure 1. For the sake of brevity, these mesogens were named **u-Az**, **p-Az**, **u-phAz**, and **p-phAz**, where u and p refer to the **u**ndecenyloxy and **p**entenoate flexible chain, respectively. Az and phAz correspond to the **az**obenzene and **ph**enylenazobenzene rigid unit, respectively. The precursors were prepared through several reactions such as azo-coupling (I-1 and I-5), Williamson (I-2), aryl-boronation (I-3) and Suzuki-Miyaura cross-coupling (I-4); some of them reported in previous works [10–12]. **u-phAz** and **u-Az** were obtained through a Williamson reaction by reacting 11-bromoundecene with I-4 and I-5, respectively. **p-phAz** and **p-Az** were prepared through an esterification reaction by combining pentenoyl chloride with I-4 and I-5, respectively.

4-decyloxy-4′-(4-hydroxyphenyl)-azo)-[1,1′-biphenyl]-3-carbonitrile (I-4)

In a 250 mL two-neck round-bottom flask, equipped with stirring and Argon atmosphere, 1.51 g (5.45 mmol) of I-1, 1.5 g (4.95 mmol) of I-3 and 100 mL of THF were introduced. The mixture was stirred and heated to 65°C. Next, 0.11 g (0.10 mmol) of tetrakis (triphenyl phosphine) palladium [0] and 37.5 mL (75 mmol) of Na_2CO_3 2M were added, and the reaction proceeded for about 84 h. Then, the reaction was allowed to cool to room temperature and the organic phase was subsequently dispersed in HCl (10 wt%), washed until neutral pH, and dried overnight. The crude product was purified in a chromatographic column using two different eluent solutions: in a first stage hexanes-ethyl acetate [80:20] and in a second stage THF-hexanes [40:60]. Finally, the brown-yellow powder (I-4) was dried overnight (yield 84.8%). ^1H NMR (500 MHz, $CDCl_3$, $\delta = ppm$): 0.89 (t, $J = 6.78$ Hz, 3H, CH_3); 1.21–1.59 (m, 26H, CH_2); 1.85 (m, 4H, CH_2, α CH_2–Oph); 2.05 (m, 2H, CH_2, α $C = C$) 4.12 (t, $J = 6.47$ Hz, 2H, CH_2, α O-ph); 5.07 (s, 1H, OH); 6.96 (d, $J = 9.14$ Hz, 2H, Ar-H, *o*-OH); 7.05 (d, $J =$ 8.83 Hz, 1H, Ar–H, *o*-OCH_2, *m*-CN); 7.63 (d, $J = 8.51$ Hz, 2H, Ar–H, *o*-ph, *m*-$N = N$); 7.78

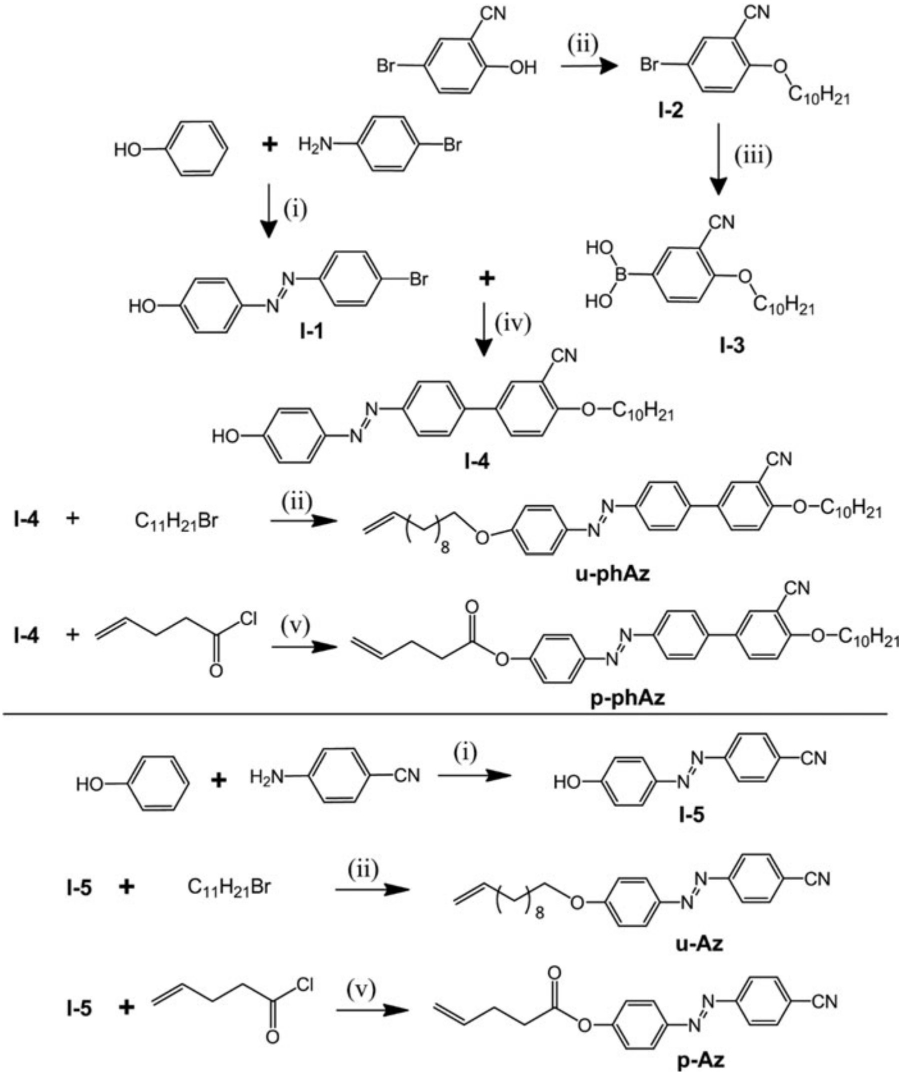

Figure 1. Synthesis route for the preparation of the vinyl-functionalized mesogens **u-Az**, **p-Az**, **u-phAz**, and **p-phAz**. (i) $NaNO_2$, HCl; NaOH, (ii) K_2CO_3, KI, acetone, 65°C, (iii) BuLi/THF; $B[OCH(CH_3)_2]_3$; HCl 2M, (iv) $Pd(PPh_3)_4$/THF/Na_2CO_3 2M, 65°C, (v) $CHCl_3$/TEA, 40°C.

(d, $J = 8.83$ Hz, 1H, Ar–H, *o*-ph, *p*-CN); 7.83 (s, 1H, Ar–H, *o*-CN, *m*-OCH_2); 7.93 (d, $J = 8.51$ Hz, 2H, Ar–H, *o*-N = N, *m*-OH); 7.95 (t, $J = 8.83$ Hz, 2H, Ar–H, *o*-N = N, *m*-ph). FT-IR (KBr, cm^{-1}) 3329 (s, ν_{as} OH), 2923 (s, ν_{as} CH_2); 2851 (m, ν_s CH_2); 2240 (m, ν C≡N); 1606, 1586, 1490, 1465 (m, ν_s ph); 1285 (s, ν_{as} C-O-ph); 1138 (m, ν_{as} O–C–C); 846, 816 (s, δ CH_2).

(4-((3′-cyano-4′-decyloxy)-[1,1′-biphenyl]-4-azo-)-phenyl pent-4-enoate (p-phAz)

In a 25 mL Schlenk tube 1.0 g (2.2 mmol) of I-4, 5 mL of chloroform, and 2 mL of triethylamine were introduced. The solution was stirred and heated at 40°C before adding 0.286 g (2.42 mmol) of 4-pentenoyl chloride, and then, the reaction was allowed to proceed for about 48 h. Next, all solvents were evaporated, and the solid was dried and thoroughly washed with ethanol. Finally, the mesogen **p-phAz** obtained as a brown-yellow powder was dried overnight

(Yield: 86.4%). ^{1}H NMR (500 MHz, $CDCl_3$, δ = ppm): 0.82 (t, J = 6.78 Hz, 3H, CH_3); 1.15–1.55 (m, 14H, CH_2); 1.81 (q, J = 7.01 Hz, 2H, CH_2); 2.47 (m, 2H, CH_2, α C = C); 2.65 (t, J = 7.26 Hz, 2H, CH_2, α COO); 4.06 (t, J = 6.62 Hz, 2H, CH_2, α OAr); 5.06 (m, 2H, CH_2, α (CH =)); 5.85 (m, 1H, CH, α (CH_2 =)); 6.98 (d, J = 8.83 Hz, 1H, Ar–H, *o*-OCH_2, *m*-CN); 7.18 (d, J = 8.82 Hz, 2H, Ar–H, *o*-OCO); 7.58 (d, J = 8.2 Hz, 2H, Ar–H, *o*-ph, *m*-N = N); 7.72 (d, J = 8.83 Hz, 1H, Ar–H, *o*-ph, *p*-CN); 7.77 (s, 1H, Ar–H, *o*-CN, *m*-OCH_2); 7.91 (d, J = 5.67 Hz, 2H, Ar–H, *o*-N = N, *m*-ph); 7.93 (t, J = 6.31 Hz, 2H, Ar–H, *o*-N = N, *m*-OCO). FT-IR (KBr, cm^{-1}) 3071 (w, ν_{as} C = C–H); 2923 (s, ν_{as} CH_2); 2850 (m, ν_s CH_2); 2225 (m, ν C≡N); 1757 (s, ν_{as} (C = O)–O); 1639 (w, ν_{as} C = C–H); 1599 y 1490 (s, ν_s ph); 1274 (s, ν_{as} C-O-ph); 1132 (s, ν_{as} O–C–C); 851 (s, δ CH_2).

((4′-cyano-phenyl)-azo)-phenyl pent-4-enoate (p-Az)

This compound was synthesized using a similar procedure (reaction and purification conditions) to **p-phAz**. 1.0 g (4.5 mmol) of I-5, 5 mL of chloroform, 2 mL of triethylamine and 0.586 g (4.95 mmol) of 4-pentenoyl chloride. The product was obtained like an orange powder (Yield: 65.8%). ^{1}H NMR (500 MHz, $CDCl_3$, δ = ppm): 2.47 (m, 2H, CH_2, α C = C); 2.65 (t, J = 7.25 Hz, 2H, CH_2, α COO); 5.07 (m, 2H, CH_2, α (CH =)); 5.85 (m, 1H, CH, α (CH_2 =)); 7.20 (d, J = 9.14 Hz, 2H, Ar–H, *o*-OCO); 7.75 (d, J = 8.51 Hz, 1H, Ar–H, *o*-ArH, *p*-CN); 7.91 (d, J = 5.99 Hz, 2H, Ar–H, *o*-N = N, *m*-CN); 7.93 (d, J = 6.31 Hz, 2H, Ar–H, *o*-N = N, *m*-OCO). FT-IR (KBr, cm^{-1}) 3081 (w, ν_{as} C = C–H); 2924 (m, ν_{as} CH_2); 2853 (m, ν_s CH_2); 2224 (m, ν C≡N); 1771 (s, ν_{as} (C = O)–O); 1643 (w, ν_{as} C = C–H); 1586 y 1494 (m, ν_s ph); 1200 (s, ν_{as} C-O-ph); 1105 (m, ν_{as} O–C–C); 851 (s, δ CH_2).

4-(decyloxy)-4′-((undec-10-enyl-1-oxy)-phenyl)-azo)-[1,1′-biphenyl]-3-carbonitrile (u-phAz)

In a 250 mL two-neck round-bottom flask 1.0 g (2.2 mmol) of I-4, 0.36 g (2.64 mmol) of K_2CO_3, 0.04 g (0.3 mmol) of KI and 80 mL of acetone were introduced. Next, the mixture was stirred and heated to 65°C and then 0.58 mL (2.64 mmol) of 11-bromo-1-undecene were added dropwise. The reaction was allowed to proceed during 84 h. Once this period elapsed the solution was filtrated and the solid was dried. Afterwards, the product was separated in a chromatographic column (250 mL-silica gel) using hexanes-ethyl acetate [80:20] as eluent and the recuperated solid was dried. The product **u-phAz** was obtained like a yellow-brown powder (Yield: 72.3%). ^{1}H NMR (500 MHz, $CDCl_3$, δ = ppm): 0.89 (t, J = 6.78 Hz, 3H, CH_3); 1.21–1.59 (m, 26H, CH_2); 1.85 (m, 4H, CH_2, α CH_2-Oph); 2.05 (m, 2H, CH_2, α C = C); 4.04 and 4.12 (t, J = 6.47 Hz, 4H, CH_2, α O-ph); 4.97 (m, 2H, CH_2, α (CH =)); 5.81 (m, 1H, CH, α (CH_2 =)); 6.99 (d, J = 9.14 Hz, 2H, Ar–H, *o*-OCH_2); 7.05 (d, J = 8.83 Hz, 1H, Ar–H, *o*-OCH_2, *m*-CN); 7.63 (d, J = 8.51 Hz, 2H, Ar–H, *o*-ph, *m*-N = N); 7.78 (d, J = 8.83 Hz, 1H, Ar–H, *o*-ph, *p*-CN); 7.83 (s, 1H, Ar–H, *o*-CN, *m*-OCH_2); 7.93 (d, J = 8.51 Hz, 2H, Ar–H, *o*-N = N, *m*-OCH_2); 7.95 (t, J = 8.83 Hz, 2H, Ar–H, *o*-N = N, *m*-ph). FT-IR (KBr, cm^{-1}) 3054 (w, ν_{as} C = C–H); 2923 (s, ν_{as} CH_2); 2850 (m, ν_s CH_2); 2223 (w, ν C≡N); 1636 (w, ν_{as} C = C–H); 1601 y 1494 (s, ν_s ph); 1247 (s, ν_{as} C-O-ph); 1135 (m, ν_{as} O–C–C); 849 (s, δ CH_2).

4-((undec-10-enyl-1-oxy)-phenyl)-azo)-benzonitrile (u-Az)

The mesogen **u-Az** was synthesized following the same procedure as for **u-phAz**. 5.0 g (22.4 mmol) of I-5, 5.9 mL (26.9 mmol) of 11-bromo-1-undecene, 3.7 g (26.9 mmol) of K_2CO_3, 0.5 g (3 mmol) of KI and 80 mL of acetone. The purification process consisted in separate the liquid phase by filtration to be later concentrated and precipitated in methanol. The final product was recuperated by filtration to be further dried in a vacuum oven. The product was obtained like a yellow powder (Yield: 89.6%). ^{1}H NMR (500 MHz, $CDCl_3$, δ =

ppm): 1.21–1.59 (m, 12H, CH_2); 1.83 (m, 2H, CH_2, α CH_2-Oph); 2.05 (m, 2H, CH_2, α $C=C$); 4.05 (t, $J = 6.6$ Hz, 4H, CH_2, α O-ph); 4.96 (m, 2H, CH_2, α ($CH=$)); 5.81 (m, 1H, CH, α ($CH_2=$)); 7.01 (d, $J = 9.05$ Hz, 2H, Ar–H, *o*-OCH_2); 7.78 (d, $J = 8.56$ Hz, 2H, Ar–H, *o*-CN); 7.92 (d, $J = 1.5$ Hz, 2H, Ar–H, *o*-N = N, *m*-OCH_2); 7.95 (d, $J = 2.2$ Hz, 2H, Ar–H, *o*-N = N, *m*-CN). FT-IR (KBr, cm^{-1}) 3074 (w, ν_{as} C = C–H); 2919 (s, ν_{as} CH_2); 2853 (m, ν_s CH_2); 2222 (w, ν C≡N); 1639 (w, ν_{as} C = C–H); 1600 y 1498 (s, ν_s ph); 1250 (s, ν_{as} C-O-ph); 1141 (m, ν_{as} O–C–C); 841 (s, δ CH_2).

2.3. Instruments

The chemical structure of mesogens was characterized by infrared spectroscopy using a Nicolet Magna IR-550 spectrophotometer and by nuclear magnetic resonance with a Bruker Ultrashield 500 MHz spectrometer. The thermal stability was evaluated in a thermogravimetric analyzer (TGA-Q500) of TA-Instruments employing a heat rate of 10°C/min from 30 to 800°C. The thermal transitions were determined with a differential scanning calorimeter (Discovery Series) from TA-Instruments, at heating-cooling rates of 10°C/min under nitrogen atmosphere (high purity). Optical textures of these compounds were observed in an Olympus BX53 microscope equipped with a temperature controlling hot stage from Linkam and a Micropublisher 3.3 RTV Q-Imaging digital camera. The molecular stacking of mesogens was determined from the X-ray diffraction analysis. The diffraction patterns were acquired at different temperatures upon cooling from the isotropic phase, using a SWAXS from Anton Paar (SAXSess mc^2) equipped with a sample holder unit (TCS 300-C), an image plate detector, and a temperature control unit (TCU50). For the XRD analysis, each mesogen was sealed in a Hampton Research glass capillary having an outer diameter of 1.0 mm and a wall thickness of 0.01 mm. The X-rays (Cu k_α radiation; $\lambda_{max} = 0.1542$ nm) were generated at 40 kV and 50 mA.

3. Results and discussion

3.1. Synthesis and chemical structures

The chemical structure of the vinyl-functionalized mesogens was characterized by ^1H NMR and ^{13}C NMR spectroscopies. Figure 2 shows the ^1H NMR spectra of **u-phAz**, **p-phAz**, **u-Az**, and **p-Az**. The four spectra show two signals at 5.0 and 5.8 ppm corresponding to the protons of the vinyl group. The spectra of **p-phAz** and **p-Az** display a signal at 2.65 ppm which was assigned to the protons of the CH_2 group in α position to the ester group. The spectra of **u-phAz** and **u-Az** show a signal at 4.05 ppm which was associated to protons of the CH_2 group in α position to the phenoxy group. Figure 3 shows the ^{13}C NMR spectra of **p-Az** and **u-Az**, where it is possible to observe the characteristic signals of the vinyl group at 118 (–HC = **C**H_2) and 137 ppm (–H**C** = CH_2). Other signals of functional groups are that of **C**-O at 69 for **u-Az** and that of O–**C** = O at 171 ppm for **p-Az**.

The presence of characteristic functional groups was corroborated by infrared spectroscopy as observed in the spectra depicted in Figure 4. The absorption bands were assigned as follows: 3080 and 1640 cm^{-1} stretching of vinyl groups (C = C–H); 2920 and 2850 cm^{-1} stretching of methyl and methylene groups (C-H); 2222 cm^{-1} stretching of the nitrile group (CN); 1770 cm^{-1} stretching of carbonyl group (C = O) presenting a bathochromic effect arising from its close vicinity to the nucleophilic substituent (O-ph); 1600 cm^{-1} stretching of aromatics groups (C = C–H), 1250 cm^{-1} stretching of ether groups C-O-C; 1200 cm^{-1} stretching of esters with phenyl substituent (ph–O–C = O); 1140 cm^{-1} stretching in phenylalkyl ethers (C–O–ph), and 850 cm^{-1} flexion of the C-H group [13].

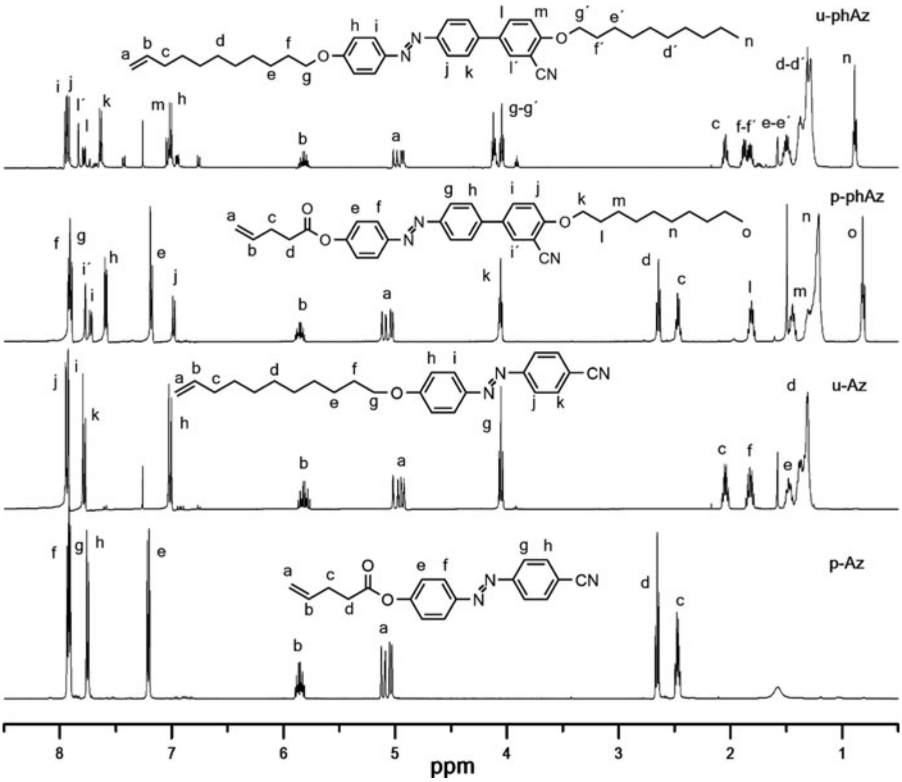

Figure 2. ^{1}H NMR spectra of vinyl-functionalized mesogens.

3.2. Thermotropic behavior

The initial decomposition temperature (2wt% lose weight) of the vinyl-functionalized mesogens is around 210°C. This temperature was taken into account for the further analysis by differential scanning calorimetry (DSC) as well as by polarizing optical microscopy and X-ray diffraction performed at variable temperature. The heating and cooling DSC thermograms

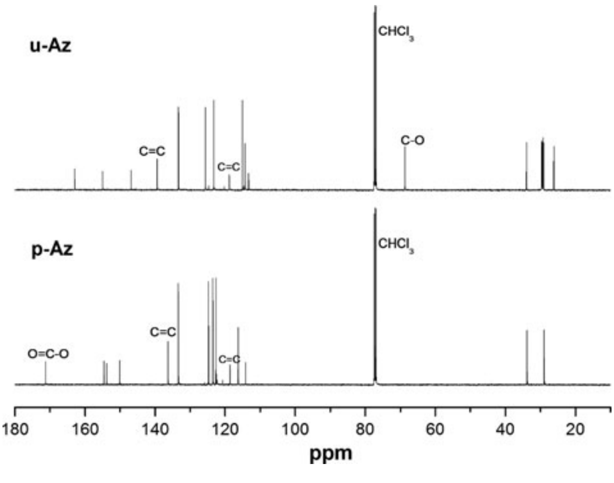

Figure 3. ^{13}C NMR spectra of the mesogens **u-Az** and **p-Az**.

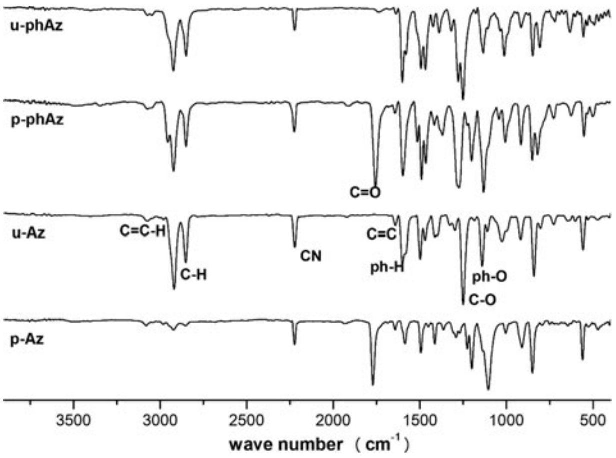

Figure 4. FT-IR spectra of vinyl-functionalized mesogens.

for mesogens are depicted in Figure 5. As it can be noted, the four mesogens display a pair of transitions (endotherms-exotherms) indicating the presence of liquid-crystalline phases. The effect of the length and rigidity of the molecules on the clearing temperature can be readily seen by comparing the short mesogens **p-Az** ($T_i = 119°C$) and **u-Az** ($T_i = 99°C$) with the long ones **u-phAz** ($T_i = 152°C$) and **p-phAz** ($T_i = 188°C$). The high temperature exotherm of **u-Az** and **p-Az** is comparatively small ($\Delta H \leq 3.7$ J/mol) and can be attributed to an isotropic-nematic transition (inset Figure 5) [14,15].

The mesomorphic behavior of the vinyl-functionalized mesogens was corroborated by polarized optical microscopy. On cooling from the isotropic state, focal-conic fan and homeotropic textures were observed for **u-phAz** (Figure 6a) and **p-phAz** (Figure 6c). For the former, a clear homeotropic to Schlieren transition was also detected (Figure 6a-b). These kind of textures and transitions are characteristics of smectic phases possessing positional and orientational order[16]. On the other hand, **p-Az** developed a Schlieren texture (Figure 6d) which was associated with a low ordered phase (nematic) while **u-Az** exhibited a dark field typical of a homeotropic behavior (molecules aligned in a perpendicular direction to the glass slides) [17].

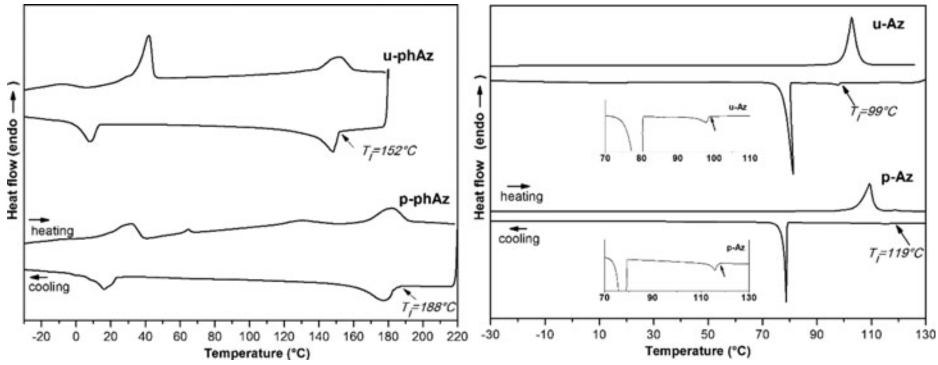

Figure 5. DSC thermograms of vinyl-functionalized mesogens obtained on heating and cooling runs.

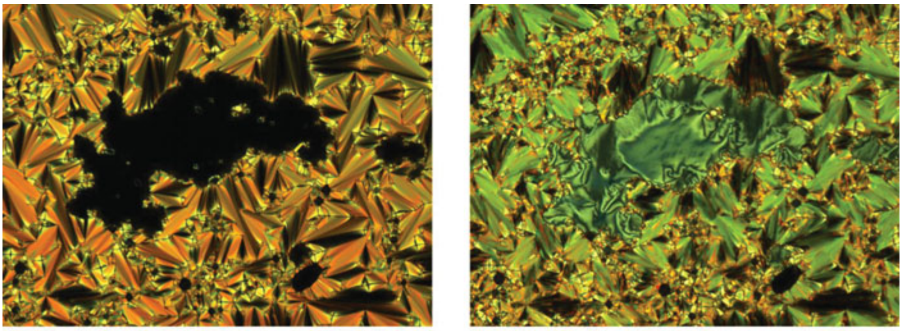

(a) **u-phAz** (145 °C) (b) **u-phAz** (137 °C)

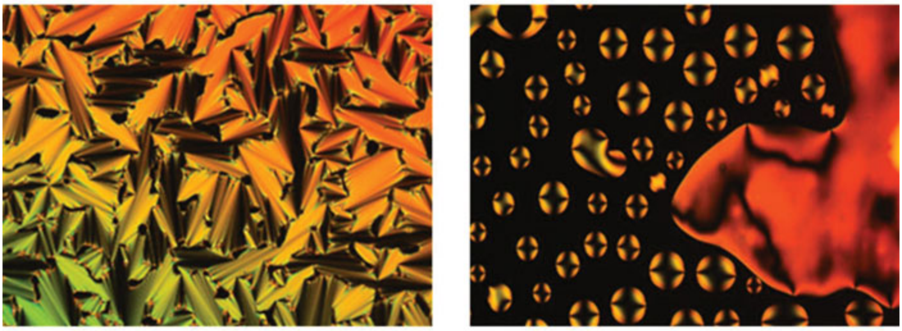

(c) **p-phAz** (170 °C) (d) **p-Az** (118 °C)

Figure 6. Optical textures for the vinyl-functionalized mesogens.

3.3. Nature and structure of mesophases

The four vinyl-functionalized mesogens were analyzed by X-ray diffraction at variable temperature, capturing diffraction patterns during the cooling process (Figure 7). The XRD patterns confirmed the presence of nematic or smectic liquid-crystalline phases for the studied mesogens. The diffractograms of **p-Az** and **u-Az** displayed only broad and weak peaks at both

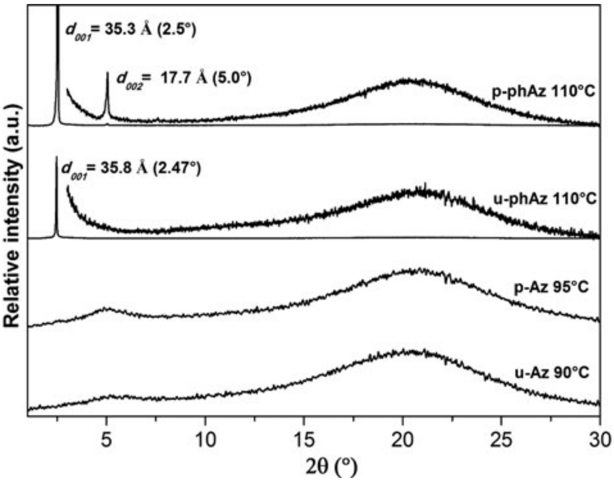

Figure 7. XRD patterns of mesogens obtained at different temperatures.

Table 1. Mesophases and their arrangement observed for the vinyl-functionalized mesogens.

Mesogen	Temperature (°C)	L (Å)	d_{001} (Å)	d/L	Mesophase[b] and transition temperature (°C)
p-Az	95	19.6	—	—	Cr 79 N 119 I
u-Az	90	27.0	—	—	Cr 80 N 99 I
p-phAz	110	34.3	35.3	1.02	Cr 24 SmA 188 I
u-phAz	110	42.3	35.8	0.85[a]	Cr 15 SmC[a] 135 SmA[C] 152 I

[a] tilt angle = 33°.
[b] Nematic (N), Smectic A (SmA), Smectic C (SmC).
[C] detected only by POM.

low and wide-angle regions ($2\theta = 20.5°$, 4.4 Å), which corroborate the presence of a nematic (N) phase. The other two mesogens **u-phAz** and **p-phAz** displayed a sharp Bragg diffraction peak (001) at 2.47 and 2.50°, respectively. This sharp peak corresponds to the layer spacing of the smectic stacking. In the wide-angle region, the broad diffraction peak (4.5Å) indicates an in plane random order of molecules, which is characteristic of fluidic or low viscous smectic phases (SmA or SmC) [18].

To determine the way the mesogens are arranged in the smectic phase, the experimental distance (d_{001}) of **u-phAz** (35.8 Å) and **p-phAz** (35.3 Å) was compared with their theoretical length in their minimal energy conformation (*L*), calculated by molecular modelling software (Spartan 14, equilibrium geometry / Hartree Fock/6–31G*). The obtained *d/L* ratios are gathered in Table 1. For **p-phAz** a *d/L* ratio close to unity corresponds to a monolayer arrangement, where the strong interactions between the phenylene groups may promote the molecular order inside the smectic layers. For **u-phAz** the *d/L* ratio is around 0.85, also indicating a monolayer arrangement but with mesogens tilted with respect to the smectic plane, characteristic of a Smectic C (SmC) phase [19]. POM results indicated that **u-phAz** first develops a Smectic A phase from the isotropic state, which then undergoes a transition towards a paramorphotic Smectic C phase. Such transition, registered by POM in a short temperature interval, was no detected neither by DSC nor by XRD. The mesomorphic sequence for each one of the mesogens can be seen in Table 1.

The vinyl-functionalized liquid crystals synthesized in this work are materials possessing a chromophore azobenzene group that can be photo-isomerized with linearly polarized light to achieve aligned molecular domains [20]. These monomeric mesogens can be polymerized via free radical polymerization or grafted onto poly-hydrosiloxanes in order to obtain side-chain liquid crystal polymers (SCLCP) and elastomers (SCLCE) [21]. The photo-triggerable liquid crystal elastomers are being intensely explored for photo-mechanical and thermo-mechanical actuation [22].

4. Conclusions

The four synthesized vinyl-functionalized azobenzene mesogens showed a mesomorphic behavior. These mesogens exhibit a relatively high thermal stability and a mesomorphism that extends over a broad temperature range, particularly those having an extra phenyl group. The mesogens having a CN-azobenzene core (**p-Az** and **u-Az**) develop a nematic phase with a clearing temperature that decreases by increasing the length of the flexible segment. The molecules carrying the long CN-phenyleneazobenzene core (**p-phAz** and **u-phAz**) exhibit a higher clearing temperature and develop smectic phases. The mesogen **p-phAz** showed only an orthogonal smectic phase (SmA) where the long rigid cores may have strong lateral interactions. Respect to **u-phAz**, this developed orthogonal (SmA) and tilted (SmC) monolayer arrangements. The vinyl-functionalized mesogens here studied can be used for the synthesis of side-chain liquid crystal elastomers with potential application in photo-mechanical or thermo-mechanical actuation systems.

Acknowledgments

The authors thank Guadalupe Méndez, Dinorah Rodríguez, Jorge L. Robles, and Jorge F. Espinoza for their helpful technical assistance.

Funding

This research project was supported by CONACYT (157652-Y and 258195) México.

References

[1] Pelzl, G., & Weissflog, W. (2007). in *Thermotropic Liquid Crystals*, edited by Ramamoorthy, A., Springer; Berlin.
[2] Goodby, J. W., Gray, G. W., Demus, D., Goodby, J., Gray, G. W., Spiess, H. W., & Vill, V. (2008). in *Handbook of Liquid Crystals Set*, Wiley-VCH Verlag GmbH; pp. 17.
[3] Wang, X.-J., & Zhou, Q.-F. (2004). *Liquid Crystalline Polymers*, World Scientific Publishing; Singapore, pp. 1–3.
[4] García-Amorós, J., & Velasco, D. (2012). *Beilstein Journal of Organic Chemistry*, *8*, 1003.
[5] Koshima, H., Ojima, N., & Uchimoto, H. (2009). *Journal of the American Chemical Society*, *131*, 6890.
[6] Demus, D., Demus, D., Goodby, J., Gray, G. W., Spiess, H. W., & Vill, V. (2008). in *Handbook of Liquid Crystals Set*, Wiley-VCH Verlag GmbH; pp. 133.
[7] Yu, H., & Li, Q. (2013). in *Intelligent Stimuli-Responsive Materials*, John Wiley & Sons, Inc.; pp. 233.
[8] Lee, K. M., & White, T. J. (2012). *Macromolecules*, *45*, 7163.
[9] Garcia-Amoros, J., Martinez, M., Finkelmann, H., & Velasco, D. (2014). *Physical Chemistry Chemical Physics*, *16*, 8448.
[10] García, T., Larios-López, L., Rodríguez-González, R. J., Martínez-Ponce, G., Solano, C., & Navarro-Rodríguez, D. (2012). *Polymer*, *53*, 2049.
[11] Gutiérrez-Cuevas, K. G., Larios-López, L., Rodríguez-González, R. J., Donnio, B., & Navarro-Rodríguez, D. (2013). *Liquid Crystals*, *40*, 534.
[12] Altomare, A., Andruzzi, L., Ciardelli, F., Gallot, B., & Solaro, R. (1998). *Polymer International*, *47*, 419.
[13] Silverstein, R. (2005). *Spectroscopy Identification of Organic Compounds* (7th Edn.), Wiley; United States, pp. 550.
[14] Nishiya, W., Takanishi, Y., Yamamoto, J., & Yoshizawa, A. (2014). *Journal of Materials Chemistry C*, *2*, 3677.
[15] Paterson, D. A. et al. (2016). *Journal of the American Chemical Society*, *138*, 5283.
[16] Dierking, I. (2003). *Textures of Liquid Crystals*, Manchester U.K., pp. 233.
[17] Prasad, V., Kang, S.-W., Suresh, K. A., Joshi, L., Wang, Q., & Kumar, S. (2005). *Journal of the American Chemical Society*, *127*, 17224.
[18] Seddon, J. M., Demus, D., Goodby, J., Gray, G. W., Spiess, H. W., & Vill, V. (2008). in *Handbook of Liquid Crystals Set*, Wiley-VCH Verlag GmbH; pp. 635.
[19] García, T., Larios-López, L., Rodríguez-González, R. J., Torres-Lubián, J. R., & Navarro-Rodríguez, D. (2012). *ChemPhysChem*, *13*, 3937.
[20] Yager, K. G., & Barrett, C. J. (2006). *Journal of Photochemistry and Photobiology A: Chemistry*, *182*, 250.
[21] Agrawal, A., Adetiba, O., Kim, H., Chen, H., Jacot, J. G., & Verduzco, R. (2015). *Journal of Materials Research*, *30*, 453.
[22] de Jeu, W. H. (2012). *Liquid Crystal Elastomers: Materials and Applications*, Springer Verlag;Berlin, pp. 239.